Developments and Upgrades of Linac

High Power RF Backup System [9]

The linac is equipped with thirteen 80 MW pulse klystrons (E3712, Toshiba Electron Tubes & Devices Co.,Ltd). All the klystrons are feeding RF power (10 pps) to the accelerating structures, and two are intermittently disabled by the trigger system in synchrony with the beam trigger signals (1 pps) to avoid beam accelerations. That is, eleven of the klystrons have usually been used to accelerate electron beams to 1 GeV, and the other two have been kept for hot spares on line.

Except for the primary and ECS's klystrons, when one of the eleven working klystrons fails and it cannot recover within a few minutes, a standby klystron is activated to accelerate the beams instead of the failed one. A serious failure of the primary klystron, however, completely stops the linac operation for a long time because it feeds RF power to the injector section of the linac and the long drive line for the other eleven klystrons.

We therefore constructed a backup system for the primary klystron to feed RF power from the second klystron to the injector, as shown in Fig. 12. The backup system is composed of waveguide circuits, a high-power waveguide switch, and its control system. The waveguide switch, the key component of this system, was developed based on the design of a commercial waveguide switch manufactured by Nihon Koshuha Co., Ltd.

High-power waveguide switches (rotary E-bend type) are widely used in accelerators but most are used in SF_6 gas. In the SPring-8 linac, high-power waveguides are used in a vacuum except for the bunching section. Therefore, a vacuum-type waveguide switch is preferred for this backup system. A 10 MW waveguide switch used in a vacuum has been developed by Nihon Koshuha Co., Ltd. We improved this waveguide switch to transmit higher peak and average RF power. Relevant improvements are listed below:

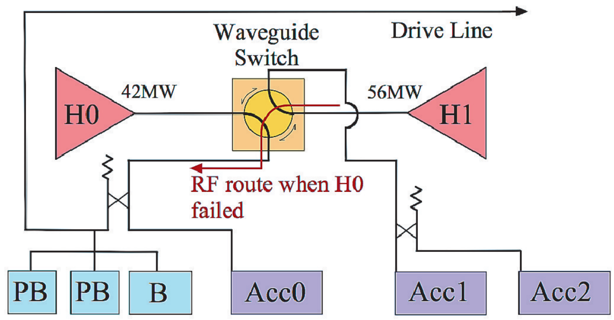

Fig. 12. New backup system for primary klystron H0.

- The bonding method for the rotor (material: OFC C1011, Hitachi Cable, Ltd.), fabricated in halves, was changed from bolt connection to diffusion bonding. This prevents air voids between bonding surfaces and contributes to UHV stability.
- The surface of the rotor was processed by an electropolishing method to remove microstructures and minimize the possibility of vacuum RF discharges in the waveguide switch.
- A rotor cooling system was fabricated as illustrated in Fig. 13. A copper rod is firmly attached to the rotor to conduct the heat due to RF power loss. The rod is detached from the rotor during rotation.
- A vacuum evacuation port was added to enhance pumping speed in the choke groove and in the thermal conductor chamber.

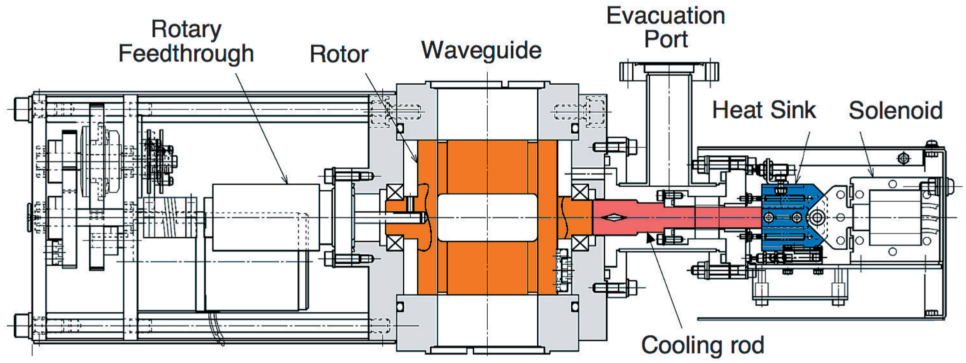

Fig. 13. Structure of waveguide switch.

After a high-power test of the waveguide switch at the RF gun test stand, in February 2006, the waveguide switch was installed between the high-power waveguide circuits of the first (H0) and second (H1) klystrons to establish the backup system.

RF conditioning was performed for seven days in the daytime with an increased repetition rate of 60 pps (normally 10 pps). After conditioning for 24 hours, the peak power of the H0 klystron reached a normal level (50 MW), and the drive power for the other klystrons became sufficient. The RF power of the second klystron reached a maximum of 74 MW after conditioning for 56 hours. Under this condition, the power loss in the rotor of the waveguide switch was estimated at 10 W, and the temperature of the heat-sink at the outer end of the thermal conductor of the waveguide switch became 42°C based on an actual measurement.

Thus, the availability and reliability of the high power RF system in the SPring-8 linac have been enhanced with the construction of this backup system. In 2007, we will install a backup electron gun to increase total reliability.

Development of Photocathode RF Gun - Laser pulse stacker forming long light pulse [10]

To minimize the beam emittance of a photocathode RF gun, the laser pulse shape should be optimized three-dimensionally. One of the candidates of reliable 3D laser pulse shape is cylindrical (spatially top-hat, and temporally rectangular pulse). In the test facility of the photocathode laser light source at SPring-8, several 3D shaping systems have been developed as a combination of spatial (transverse: x-, y-axes) and temporal (longitudinal: z-axis) pulse-shaping methods in the last 5 years. The spatial profile has been reformed with a microlens array or a deformable mirror (DM). The temporal profile has been formed with a spatial light modulator (SLM) or a light pulse stacker.

A pulse stacker forms a long light pulse by stacking short light pulses. The pulse stacker developed in SPring-8 is composed of three stages: a pulse doubler unit, which consists of a pair of polarizing beam splitters, a half-wave plate, and a movable corner reflector to adjust an optical delay. The optical system was designed to alternate s- and p-polarization in the final light pulse train in order to avoid optical interference between the adjacent light pulses, as illustrated in Fig. 14.

A pulse doubler unit works as follows: The fully s-polarization of a laser pulse is rotated to 45-degree polarization with the half-wave plate. It is divided into s- and p-polarized pulses with the first polarizing beam splitter. The p-polarized pulse is delayed with the optical delay line and then recombined with the s-polarized pulse with the second beam splitter to form a double pulse light. That is, the laser pulses of 2.5 ps were successively doubled at each stage to generate a longer pulse train. The dispersion of the downstream optical system broadens each micropulses of the pulse train and consequently results in a single rectangular shape pulse. Stacking eight micropulse in the three stages, we can obtain a 20-ps width pulse. The quality of the laser pulse stacking was verified by observing electron bunch shapes as described below.

We adjusted the optical delay lines and verified the

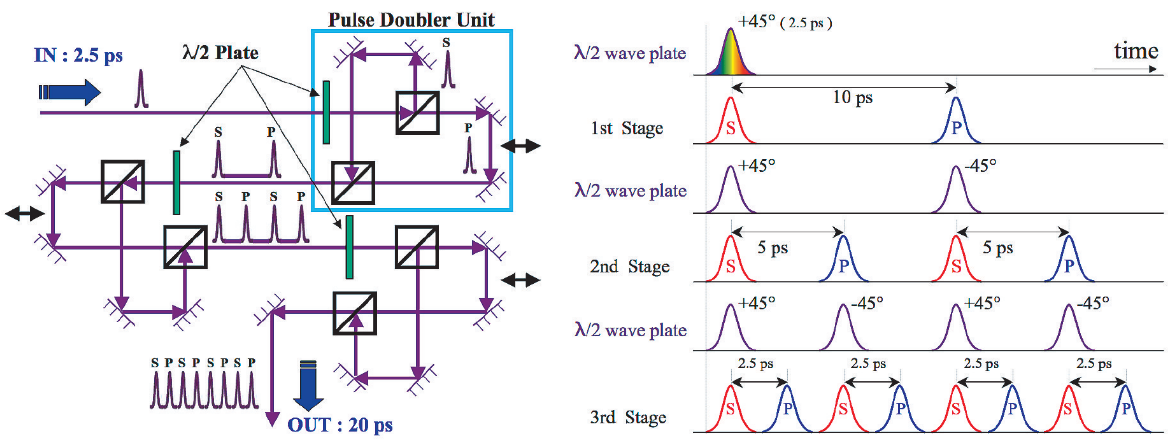

Fig. 14. Optical system (left) and timing chart (right) of UV-laser pulse stacker.

temporal profile of the stretched laser pulse, observing the projection of the temporal profile of an electron bunch as follows [11]: When the RF phase is tuned at an appropriate value to provide temporal (longitudinal) energy gradation to a bunch, the temporal distribution of the bunch is projected to the beam energy distribution which can be easily measured. Figure 15 shows examples of the beam energy distributions on a fluorescence screen downstream of a bending magnet as an energy analyzer. This method determined the absolute zeros of the optical delay lines with a good precision of about 0.5 ps, which was evaluated from the beam position jitters observed on the screen caused by the RF phase fluctuation.

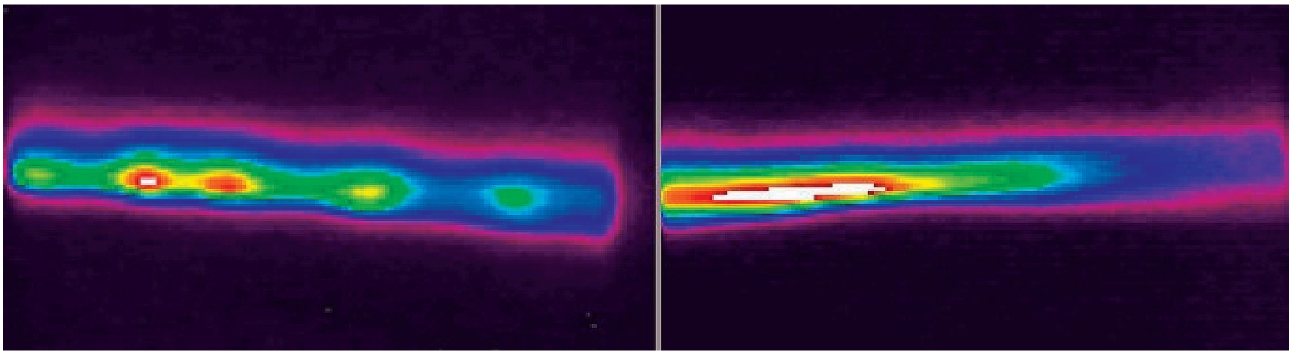

Fig. 15. Examples of the energy distributions of a 20 ps bunch on a screen monitor. The left profile in the process of optical adjustment shows discrete laser pulses, whereas the right case shows that the laser pulses were almost perfectly aligned to form a long light pulse.

Haruo Ohkuma*, Hiroto Yonehara and Hirofumi Hanaki

SPring-8/JASRI

*E-mail: ohkuma@spring8.or.jp

References

[1] T. Ohshima *et al.*: Proc EPAC2006, Edinburgh, Scotland, p.1133.
[2] H. Tanaka *et al.*: Proc. EPAC2000, Vienna, Austria, p.1086.
[3] K. Tamura *et al.*: Proc. of 1st Annual Meeting of Particle Accelerator Society of Japan and 29th Linear Accelerator Meeting in Japan, Funabashi, 2004, p.581.
[4] S. Takano *et al.*: Nucl. Instrum. Meth. A **556** (2006) 357.
[5] H. Ohkuma *et al.*: Proc. EPAC2006, Edinburgh, Scotland, p.961.
[6] Y. Suetsugu *et al.*: Proc. PAC2005, Knoxville, Tennessee, p.3203.
[7] M. Katoh: Jpn. J. Appl. Phys. **38** (1999) L547.
[8] A. Zholents *et al.*: Nucl. Instrum. Meth. A **425** (1999) 385.
[9] T. Taniuchi *et al.*: Proc. EPAC2006, Edinburgh, Scotland, p.1397.
[10] H. Tomizawa *et al.*: Russian Journal of Quantum Electronics (2007) - to be published.
[11] H. Dewa *et al.*: Proc. FEL'06, Berlin, Germany.